JPET Fast Forward. Published on August 3, 2018 as DOI: 10.1124/jpet.118.248435
This article has not been copyedited and formatted. The final version may differ from this version.

Discovery of 1-((6-aminopyridin-3-yl)methyl)-3-(4-bromophenyl)urea as a potent, irreversible myeloperoxidase inhibitor

Martin L. Marro*, Andrew W. Patterson*, Lac Lee, Lin Deng, Aimee Reynolds, Xianglin Ren, Laura Axford, Anup Patnaik, Micah Hollis-Symynkywicz, Nigel Casson, Dominique Custeau, Lisa Ames, Sally Loi, Lihe Zhang, Toshiyuki Honda, Jutta Blank, Tyler J. Harrison, Julien P.N. Papillon, Lawrence G. Hamann, Jovita Marcinkeviciene, Jean B. Regard

Cardiovascular and Metabolic Diseases (M.L.M., L.L., X.R., L.A., M.H-S., N.C., D.C., L.A., S.L., L.Z., T.H., J.M., J.B.R.), Global Discovery Chemistry (A.W.P., A.P., T.J.H., J.P.N.P., L.G.H.), PK Sciences (L.D.), Technical R&D (A.R.), Chemical Biology and Therapeutics (J.B.), Novartis Institutes for BioMedical Research, Cambridge, MA 02139 (* Equal Contribution)

JPET Fast Forward. Published on August 3, 2018 as DOI: 10.1124/jpet.118.248435
This article has not been copyedited and formatted. The final version may differ from this version.

A potent, irreversible MPO inhibitor

Jean B. Regard, Ph.D.

Novartis Institutes for Biomedical Research

22 Windsor St ; 3D310

Cambridge, MA 02139

Tel: (617)871-8567

jean.regard@novartis.com

Text pages: 29

Number of tables: 2

Number of figures: 4

Number of references: 29

Word count – abstract: 110

Word count – introduction: 753

Word count – discussion: 424

Recommended section assignment: Drug Discovery and Translational Medicine

Abstract

Myeloperoxidase (MPO) is a leukocyte-derived redox enzyme that has been linked to oxidative stress and damage in many inflammatory states, including cardiovascular disease. We have discovered aminopyridines that are potent mechanism-based, inhibitors of MPO, with significant selectivity over the closely related thyroid peroxidase. 1-((6-aminopyridin-3-yl)methyl)-3-(4-bromophenyl)urea (Aminopyridine 2) inhibited MPO in human plasma and blocked MPO-dependent vasomotor dysfunction *ex vivo* in rat aortic rings. Aminopyridine 2 also showed high oral bioavailability and inhibited MPO activity *in vivo* in a mouse model of peritonitis. Aminopyridine 2 could effectively be administered as a food admixture making it an important tool for assessing the relative importance of MPO in preclinical models of chronic inflammatory disease.

JPET Fast Forward. Published on August 3, 2018 as DOI: 10.1124/jpet.118.248435
This article has not been copyedited and formatted. The final version may differ from this version.

Introduction

Myeloperoxidase (MPO) is a heme-containing peroxidase present in phagocytic cells where it participates in the innate immune response. In neutrophils MPO is stored in azurophilic granules and it has been reported to represent 5% of total cellular protein (Schultz and Kaminker, 1962). MPO is a homo-dimeric cationic glycoprotein that binds readily to bacterial and mammalian cell surfaces. The primary anti-microbial function of MPO is achieved by catalyzing the oxidation of halides such as chloride (Cl^-) or bromide (Br-) ions by hydrogen peroxide (H_2O_2) to produce hypochlorous (HOCl) or hypobromous (HOBr) acids, respectively. Upon activation of phagocytes, MPO activity is detectable both in phagosomes and extracellularly where it can remain or transcytose into interstitial compartments and its enzymatic products can oxidize proteins, lipids, nucleic acids, and other small molecules.

Beyond clearance of pathogens, acute and chronic MPO activation is associated with generating oxidants within tissues, potentially contributing to the pathogenesis of inflammatory disease. Human DNA polymorphism associations and pharmacological data implicates aberrant MPO activity in inflammatory diseases such as cystic fibrosis, chronic obstructive pulmonary disease, Parkinson's disease, rheumatoid arthritis, acute kidney injury and atherosclerosis (Klebanoff, 2005). A role for MPO is particularly compelling in cardiovascular disease (Nussbaum et al., 2013). It has been suggested that MPO deficiency in humans is associated with a lower incidence of cardiovascular disease (Kutter et al., 2000; Rudolph et al., 2012), and MPO deficient mice are protected in a model of myocardial infarction (Askari et al., 2003). Furthermore, elevated circulating MPO levels are associated with increased cardiovascular mortality in patients

(Haslacher et al., 2012), and transgenic over-expression of MPO in hematopoietic cells exacerbates atherogenesis in mice (McMillen et al., 2005; Castellani et al., 2006).

The mechanism(s) by which MPO contributes to cardiovascular disease is not clear, but a number of hypotheses have been proposed. It has been suggested that MPO can oxidize high density lipoprotein (HDL) thereby reducing its ability to efflux cholesterol (Shao et al., 2010). Moreover, HOCl can oxidize apolipoprotein B100 leading to increased uptake of oxidized low density lipoproteins (LDL) by macrophages, potentially leading to foam cell formation (Marsche et al., 2003), a hallmark of atherosclerosis. MPO has also been suggested to impair endothelial function by consuming nitric oxide (Eiserich et al., 2002) and/or promoting endothelial apoptosis (Sugiyama et al., 2004). Finally, there is evidence to suggest that MPO can activate matrix metalloproteinases (MMPs) and inactivate tissue inhibitors of metalloproteinases (TIMPs), resulting in reduced vessel wall extracellular matrix (ECM) (Wang et al., 2007; Ehrenfeld et al., 2009). One or more of these mechanisms may play a role in atherosclerotic plaque instability and rupture, ultimately contributing to coronary artery disease, peripheral artery disease, heart failure, and stroke. Given the significant unmet medical need to treat inflammatory cardiovascular disease we undertook development of MPO inhibitors.

Mechanism-based irreversible inhibitors rely on the chemistry of the enzyme's active site and are often highly selective for the target (Copeland, 2005). MPO mechanism-based irreversible inhibition involves initial oxidation of an inhibitor by the highly oxidizing compound I form of MPO to a short-lived radical (Figure 1A). This intermediate radical can crosslink to the MPO protein or heme group, forming a covalent bond that irreversibly inhibits enzymatic activity.

JPET Fast Forward. Published on August 3, 2018 as DOI: 10.1124/jpet.118.248435
This article has not been copyedited and formatted. The final version may differ from this version.

To date, the most potent and specific MPO inhibitors that show robust *in vivo* activity are thiouracil-based, irreversible mechanism-based inhibitors (Tiden et al., 2011; Churg et al., 2012; Stefanova et al., 2012; Jucaite et al., 2015; Ruggeri et al., 2015; Zheng et al., 2015) the most advanced of which at the writing of this manuscript are AZD3241 (Johnstrom et al., 2015; Jucaite et al., 2015; Kaindlstorfer et al., 2015) (https://ncats.nih.gov/files/AZD3241-2016.pdf) and PF-06282999 (Ruggeri et al., 2015; Dong et al., 2016) (Figure 1B). In this chemotype, the thioxo functionality undergoes one-electron oxidation to generate a sulfur-based radical that crosslinks the heme group of MPO (Tiden et al., 2011; Geoghegan et al., 2012). Inhibitors from this class have advanced to clinical studies in patients for Parkinson's disease (Jucaite et al., 2015), multiple system atrophy (Clintrials.gov NCT02388295), and cardiovascular diseases (Dong et al., 2016).

Given the success of irreversible inhibitors to demonstrate *in vivo* efficacy, we sought to discover novel classes of irreversible MPO inhibitors with increased potency, selectivity against thyroid peroxidase (TPO) and suitable pharmacokinetic properties for *in vivo* testing. Here we describe the discovery of a novel chemical class of mechanism-based irreversible MPO inhibitor: the 2-aminopyridine class (i.e. Aminopyridine 1) (Figure 1B). We further describe the preclinical characterization of 1-((6-aminopyridin-3-yl)methyl)-3-(4-bromophenyl)urea (Aminopyridine 2), a potent and selective MPO inhibitor with high oral exposure and *in vivo* activity.

JPET Fast Forward. Published on August 3, 2018 as DOI: 10.1124/jpet.118.248435
This article has not been copyedited and formatted. The final version may differ from this version.

Materials and Methods

Synthesis of 2-Aminopyridine analogues:

1-((6-aminopyridin-3-yl)methyl)-3-(3-fluorophenyl)urea (Aminopyridine 1)

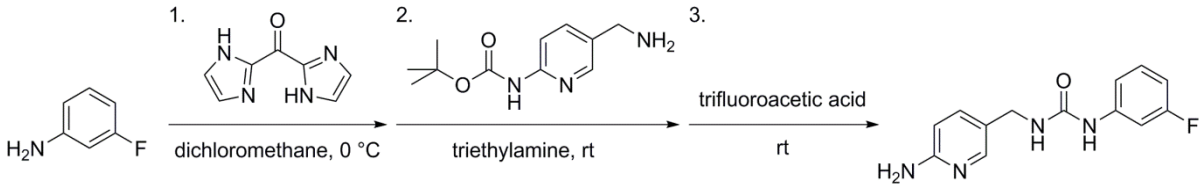

To 3-fluoroaniline (0.020 g, 0.18 mmol) in dichloromethane (1.0 mL, 0.18 M) was added carbonyldiimidazole (0.037 g, 0.23 mmol), and the solution was stirred for 30 minutes at 0 °C. Tert-butyl (5-(aminomethyl)pyridin-2-yl)carbamate (0.034 g, 0.15 mmol) and triethylamine (32 µL, 0.23 mmol) were added, and the solution was stirred at room temperature for 16 hours. Trifluoroacetic acid (1.0 mL) was added, and the solution was stirred overnight at room temperature. The reaction solution was concentrated under vacuum, and the residue was purified by preparative HPLC using a gradient of acetonitrile/H2O (0.1% NH4OH) to give 0.011 g of 1-((6-aminopyridin-3-yl)methyl)-3-(3-fluorophenyl)urea (23%). (MS (electrospray ionization) [ESI], positive ion) m/z: 261.1 (M+1); 1H NMR (400 MHz, dimethylsulfoxide-d6) δ ppm 4.08 (d, J = 5.8 Hz, 2H) 5.84 (s, 2H) 6.40 (d, J = 8.3 Hz, 1H) 6.52 (t, J = 5.7 Hz, 1H) 6.64-6.73 (m, 1H) 7.01 (ddd, J = 8.2, 1.9, 0.9 Hz, 1H) 7.23 (td, J = 8.2, 7.0 Hz, 1H) 7.32 (dd, J = 8.5, 2.5 Hz, 1H) 7.45 (dt, J = 12.2, 2.3 Hz, 1H) 7.84 (d, J = 2.0 Hz, 1H) 8.71 (s, 1H). A purity of >99% was routinely achieved (Supplemental Figure S1A).

1-((6-aminopyridin-3-yl)methyl)-3-(4-bromophenyl)urea (Aminopyridine 2)

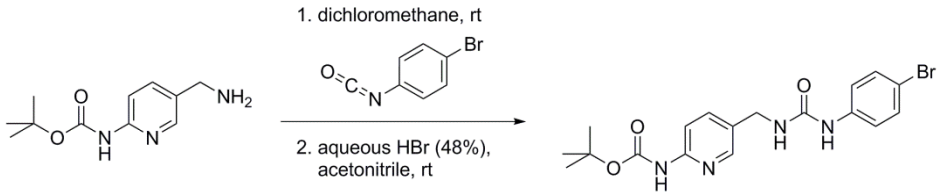

To tert-butyl (5-(aminomethyl)pyridin-2-yl)carbamate (0.190 g, 0.851 mmol) in dichloromethane (6 mL, 0.14 M) was added 1-bromo-4-isocyanatobenzene (0.169 g, 0.851 mmol), and a white precipitate formed immediately. The mixture was stirred at room temperature for 30 min and then concentrated. The resulting white solid was then suspended in acetonitrile (2 mL, 0.43 M), aqueous HBr (48%, 1 mL) was added, and the mixture was stirred at room temperature for 15 hours. The solution was then made basic with saturated aqueous ammonium hydroxide, and the resulting solid was collected by vacuum filtration washing with water and acetonitrile. Further drying under vacuum yielded 0.214 g of 1-((6-aminopyridin-3-yl)methyl)-3-(4-bromophenyl)urea (77%) as a white solid. (MS [ESI], positive ion) m/z: 321.0 (M+H), 323.0 (M+H); 1H NMR (400 MHz, dimethylsulfoxide-d6) δ ppm 4.08 (d, J = 5.7 Hz, 2H), 5.84 (s, 2H), 6.41 (dd, J = 8.6, 0.8 Hz 1H), 6.49 (t, J = 5.8 Hz, 1H), 7.29-7.43 (m, 5H), 7.84 (d, J = 2.3 Hz, 1H), 8.63 (s, 1H); ESI-HRMS: m/z calculated for C13H14N4OBr [M+1]: 321.0351; found: 321.0340]. A purity of >99% was routinely achieved (Supplemental Figure S1B).

MPO peroxidation assay: In a black 384-well plate (Costar #3573) we combined 10 mM phosphate buffer (pH 7.4) with human MPO (Cell Sciences #CSI19692), Amplex Red (ThermoFisher #A12222), and H_2O_2 to final concentrations of 2.5 nM, 10 µM, and 6.7 µM, respectively. MPO inhibitor compounds were added from a DMSO stock and the reactions were read on a SpectraMax fluorescence plate reader (Molecular Devices, Sunnyvale, CA; Ex 563 nm/Em 587 nm). Endpoint relative fluorescence units were measured at 180 seconds to calculate inhibition curves and the remaining MPO activity was calculated as %Activity = [(read-min)/(max-min)]*100.

TPO peroxidation assay: In a black 384-well plate (Costar #3573) we combined 10 mM phosphate buffer (pH 7.4) with human TPO (Cell Sciences #CSI11064), Amplex Red (ThermoFisher #A12222), and H_2O_2 to final concentrations of 25 nM, 20 µM, and 6.7 µM, respectively. MPO inhibitor compounds were added from a DMSO stock and the reactions were read on a SpectraMax fluorescence plate reader (Molecular Devices; Ex 563 nm/Em 587 nm). Endpoint relative fluorescence units were measured at 180 seconds to calculate inhibition curves and the remaining TPO activity was calculated as %Activity = [(read-min)/(max-min)]*100.

Reversibility by dialysis: Human MPO (Lee Biosciences #426-10), MPO inhibitor (from a DMSO stock), and H_2O_2 were combined with 100 mM phosphate buffer (pH 7.4) to final concentrations of 1 µM, 20 µM, and 30 µM, respectively. Following a 10 minute reaction time 100 µM ascorbic acid was added to quench the reaction, which was then cassette dialyzed (Thermo Scientific #66383) for 72 hours in 0.5 L of 100 mM phosphate buffer (pH 7.4). Residual MPO activity could be determine by performing a 1 to 200 dilution of the dialyzed sample (5 nM MPO final concentration) into 10 mM phosphate buffer (pH 7.4) containing 10 µM Amplex Red and 6.7 µM H_2O_2. Reactions were then read using a SpectraMax M5e plate reader (Molecular Devices; Ex 563 nm/Em 590 nm) and all experiments were performed in duplicate.

Stopped flow (k_{inact}/K_i): Experiments were performed on a Stopped Flow Instrument (Kintek, Snow Shoe, PA) with 3 syringes, each allowing equal volume mixing of 40 nM MPO, 40 µM H_2O_2/40 µM Amplex Red, and variable concentration of aminopyridine in DMSO. Fluorescence was monitored for 5 second after mixing (Ex 563 nm/Em 587 nm) recording 4-5 replicates at each compound concentration. The early, linear fluorescence

JPET Fast Forward. Published on August 3, 2018 as DOI: 10.1124/jpet.118.248435
This article has not been copyedited and formatted. The final version may differ from this version.

values were fit to this equation: $[P]=V_i/k_{obs}[1 - \exp(-k_{obs}t)]$, where P is the product, V_i is the initial reaction velocity (RFU/sec), t is time (sec) and k_{obs} is the first order rate constant of enzyme inactivation. k_{obs} data were then fit to the equation $k_{obs} = (k_{inact}*[I])/(K_i + [I])$, where [I] is the inhibitor concentration in order to determine k_{inact}/Ki.

Partition ratio (k_3/k_4): To eliminate chloride salt, human MPO (Lee Biosciences #426-10) was dialyzed with a 500-fold excess volume of 100 mM phosphate buffer (pH 7.4) for 8 hours, and this was repeated two additional times. 100 nM MPO, 0.53 mM H_2O_2, and aminopyridine were incubated in 100 mM phosphate buffer (pH7.4) at room temperature for 10 minutes. 1 µL of this MPO/H_2O_2/compound solution was then added to a 384-well plate (Costar #3573) along with 99 µL of a solution containing 10.1 µM Amplex Red and 10.1 µM H_2O_2 in 10 mM phosphate buffer (pH 7.4). The plate was read on a SpectraMax fluorescence plate reader (Molecular Devices; Ex 563 nm/Em 587 nm) recording five 75 second reads each (total 300 seconds), only the initial rate was used for analysis. Remaining MPO activity was calculated as %Activity = [(read-min)/(max-min)]*100, and %Activity was plotted as a function of the ratio [inhibitor]/[MPO] in XLFit (Microsoft Excel). The point at which the % Activity becomes zero indicates the number of moles of inhibitor required to inactivate one mole of enzyme (1+r). This value was used to determine the partition ratio r.

MPO plasma assay: This assay is conceptually similar to one previously published (Franck et al., 2009). Briefly, 96-well Protein G-coated plates (Reacti-Bind, Pierce #15157) were washed with 150 mM NaCl + 0.1% Tween-20 (wash buffer pH 7.4) and incubated at room temperature with either anti-mouse MPO antibody (R&D Systems AF3667, 5 µg/mL) or anti-human MPO antibody (R&D Systems AF3174, 5 µg/mL) in

100 µL Superblock buffer with 0.05% Tween-20 (Pierce #37535) for 2 hours. Wells were washed four times with PBS buffer (pH 7.4). For MPO IC_{50} studies 1 nM MPO, 1 mM H_2O_2 and compound in increasing concentrations was mixed with heparinized human plasma (isolated from healthy volunteers, pooled from n=10 donors) and 100µL was added per well. The plate was then incubated at 37 ºC for 2 hours. The plates were washed again four times with wash buffer, and 100 µL of detection reagent [50 mM phosphate buffer (pH 7.4), 40 µM Amplex ultra-red (Life Technologies #A36006), 10 µM H_2O_2, 10 mM sodium nitrite] were added to each well and the plate was read on a SpectraMax M5e plate reader (Molecular Devices; Ex 563 nm/Em 590 nm). Under these conditions data was linear for at least 40 minutes.

Heme modification: To eliminate chloride salt human MPO (Lee Biosciences #426-10) was dialyzed with three exchanges of 500-fold excess volume of 100 mM phosphate buffer (pH 7.4) for a total of 24 hours. UV-Vis absorption spectra (Cary 50, Agilent Technologies) of MPO (1 µM) was recorded as a baseline and then 20 µM of Aminopyridine 2 was added, followed by 30 µM of H_2O_2 and 1 mM of ascorbic acid. The absorption spectrum was then measured again after a 10 minute incubation in a 1 cm path length cell.

Pharmacokinetic studies: All experiments involving animals were conducted in our AAALAC-accredited facilities, in accordance with the Guide for the Care and Use of Laboratory Animals as adopted and promulgated by the U.S. National Institutes of Health and were approved by the Novartis Animal Care and Use Committee. C57BL/6 mice or Sprague-Dawley rats (Harlan Labs, Indianapolis, IN) were administered compound either intravenously (1 mg/kg; a solution in 30%PEG300, 10% Crem EL, in

PBS) or by oral gavage (10 mg/kg; a suspension in 0.1% Tween-80, 0.5% methylcellulose in water). Similarly, purpose-bred beagle dogs were administered compound either intravenously (0.3 mg/kg; 10% 0.1N HCl, 20%PEG300, 10% Solutol, in PBS) or by oral gavage (10 mg/kg; 0.5%Tween-80/0.5% methyl cellulose, in water). Blood was collected in EDTA-coated capillary tubes. Plasma was isolated by centrifugation and frozen until analysis. Samples were prepared by liquid-liquid extraction and analyzed by liquid chromatography-tandem mass spectrometry (LC-MS/MS) and concentrations of Aminopyridine 2 were determined by interpolation from a standard curve.

Aortic ring relaxation: Male Sprague-Dawley rats (Charles River, Wilmington, MA) were purchased at eight weeks of age, housed two per cage under normal light cycle conditions (12 hours on, 12 hours off) and used within six weeks of arrival. Rats were anesthetized by isoflurane inhalation, euthanized by exsanguination and the thoracic aorta was then isolated and transferred into modified Krebs-Henseleit buffer (KHB; 1.2 mM KH_2PO_4, 27.2 mM $NaHCO_3$, 119 mM NaCl, 4.6 mM KCl, 1.75 mM $CaCl_2$, 1.2 mM $MgSO_4$, 11.1 mM glucose, 0.03 mM Na_2EDTA). The aortae were then cleaned of fat and connective tissue, cut into 2-3 mm rings and washed five times in KHB. Rings were then placed into KHB with 500 nM human MPO, 94 mM H_2O_2, and Aminopyridine 2 and incubated at 37 ºC for 45 minutes. The rings were then washed an additional five times with KHB, and mounted onto an organ bath/isometric transducer chamber (Radnoti, Monrovia, CA). Following equilibration the rings were pre-contracted with 1 µM phenylephrine, and their ability to relax with increasing amounts of acetylcholine was

assessed. As a final step 30 nM sodium nitroprusside was added to each bath to confirm normal smooth muscle cell function.

Mouse peritonitis: Male C57BL/6j or MPO null mice (Brennan et al., 2001) (both from Jackson Laboratories, Bar Harbor, ME) were purchased at eight weeks of age, housed four per cage under normal light cycle conditions (12 hours on, 12 hours off) and used within six weeks of arrival. At time zero, peritonitis was induced by injection i.p. with 1 mL of thioglycolate broth (4% in water; Sigma T9032). After 19 hours, the mice were administered an Aminopyridine 2 suspension in vehicle or vehicle (0.5% methyl cellulose, 0.1% tween-80, in water) by oral gavage. One hour later the mice were injected i.p. with 0.5 mL zymosan A (10 mg/mL in water; Sigma Z4250), and were euthanized after an additional four hours with carbon dioxide. Blood was drawn by cardiac puncture into heparinized tubes, and the plasma was isolated. The peritoneal cavity was flushed by lavage with 1.5 mL of ice-cold PBS containing 1 mM methionine and 0.01 mg/mL catalase. For chronic studies, Aminopyridine 2 was formulated into a western diet (Research Diets D12079B) at 0.0417% (~50 mg/kg/day) or 0.1668% (~200 mg/kg/day) and fed to the mice for two weeks prior to the induction of peritonitis as described above.

3-Chlorotyrosine and tyrosine quantification: Peritoneal exudate (200 µL) was placed on an Amicon 3000 MW cutoff filter and centrifuged at 14,000 x *g* for 60 minutes at 4ºC. 40 µL of the filtrate was added to a new 1.5 mL Eppendorf tube followed by 5 µL of a 500 nM solution of $^{13}C_6$-tyrosine and $^{13}C_6$-chlorotyrosine (Cambridge Isotope Laboratories) internal standard and 35 µL of borate buffer (200 mM borate in water, ~pH 8.4) and then mixed by vortexing at moderate speed for 10 seconds. A final reaction of a 100 µL

volume was achieved by adding 20 µL of derivatization reagent (6-aminoquinolyl-N-hydroxysuccinimidyl carbamate from Waters AccQ-Tag Ultra Derivatization Kit). The tube was vortexed at moderate speed for 10 seconds, and then incubated at 55 ºC in a heating block for 10 minutes. Chlorotyrosine and tyrosine were quantified on a Shimadzu LC-coupled AB Sciex Q-Trap 6500 mass spectrometer using the peak area ratio relative to the internal standards and multiplied by 62.5 as an isotopic abundance factor. Additional technical details are provided in the supplemental information.

Statistical analysis: Statistical tests used are indicated in the text and figure legends. *$P<0.05$*, *$P<0.01$*, *$P<0.001$*.

Results

More than 1.4-million compounds were screened in a fluorescent MPO peroxidation biochemical assay with the goal of identifying MPO inhibitors. This screen and follow-up efforts yielded 4669 hits that were selected for mechanism of action and selectivity profiling. IC_{50} measurements were conducted with both MPO and TPO, a close homologue of MPO. Dilution experiments were designed to identify compounds that would inhibit MPO at 20 µM compound concentration and retain inhibition after 1000-fold dilution (a behavior typical of irreversible inhibitors), and 133 compounds were identified that retained >50% inhibition of MPO activity.

One novel class of mechanism-based irreversible inhibitors that met the criteria of having an MPO IC_{50} <0.5 µM, >100-fold selectivity against TPO, and irreversible inhibition confirmed by dialysis shared a 5-substituted-2-aminopyridine pharmacophore (i.e. Aminopyridine 1) (Figure 1B). Aminopyridine 1 had a promising profile, with the rate of MPO inactivation (k_{inact}/K_i: 14,000 $M^{-1}s^{-1}$) matching that of clinical compound PF-06282999 (k_{inact}/K_i: 11,749 $M^{-1}s^{-1}$) (Ruggeri et al., 2015) (Figure 1B) and the apparent MPO IC_{50} (0.45 µM) matching that of clinical compound AZD3241 (0.63 µM) (https://ncats.nih.gov/files/AZD3241-2016.pdf) (Figure 1B), and having >200-fold selectivity over TPO (Table 1). The partition ratio (k_3/k_4) of Aminopyridine 1, which measures efficiency of irreversible inhibition, was moderate (57). Thus, reducing k_3/k_4 and increasing k_{inact}/K_i while maintaining selectivity over TPO, along with obtaining *in vivo* exposure, became the primary foci of our medicinal chemistry efforts. Optimization efforts resulted in Aminopyridine 2**,** which has a 4-bromo substituted phenyl ring in place of the 3-fluoro substitution on Aminopyridine 1 (Figure 1B). This small change provided

JPET Fast Forward. Published on August 3, 2018 as DOI: 10.1124/jpet.118.248435
This article has not been copyedited and formatted. The final version may differ from this version.

a marked improvement on MPO k_{inact}/K_i (76,500 $M^{-1}s^{-1}$) and k_3/k_4 (11) kinetic values, while further increasing to >588-fold selectivity over TPO (Table 1). Aminopyridine 2 inhibited MPO peroxidase activity *in vitro* and in human plasma MPO activity *ex vivo* with apparent IC_{50}s = 0.16 and 1.9 µM, respectively (Figure 2A).

Analysis for the activity of AP-2 against additional oxidase targets found activity against eosinophil peroxidase (EPO, with an apparent IC_{50}=0.29µM) (Supplemental Figure S2), but no apparent activity against cyclooxygenase 1, cyclooxygenase 2, cytochrome P450 3A4, cytochrome P450 2D6, cytochrome P450 2C9, monoamine oxidase A, arachidonate 12-lipoxygenase or arachidonate 5-lipoxygenase (data not shown).

The mechanism of inhibition was investigated by incubating Aminopyridine 2 (or DMSO alone) with MPO and H_2O_2 followed by dialysis and further dilution prior to analysis for MPO activity. Aminopyridine 2-dependent inhibition persisted following dialysis and dilution suggesting an irreversible mechanism (Figure 2B). The mechanism of MPO inhibition was further evaluated by plotting k_{obs} values relative to the concentration of Aminopyridine 2, allowing a determination of k_{inact} rate of 2.2/sec and K_i of 24 µM. Saturation was observed, indicating a two-step mechanism of inactivation (Figure 2C). Furthermore, Aminopyridine 2 can form conjugates with 5,5-dimethyl-1-pyrroline N-oxide (DMPO) in the presence of MPO and H_2O_2, consistent with the mechanism of inhibition involving an active radical intermediate (Supplemental Table T1).

To better understand the role of the heme moiety during inhibition, we explored the distinct spectral properties of the redox intermediates of MPO. When Aminopyridine 2 was added directly to MPO, no change in UV-Vis absorption spectrum was observed. Upon addition of H_2O_2, however, the Soret band shifted from 430 nm to 457 nm.

Additionally, the second heme specific peak at 570 nm shifted to 624 nm (Figure 2D). The addition of ascorbic acid, which would normally reduce the higher heme oxidation states back to the native Fe(III) state, did not cause a shift back to 430 nm and 570 nm indicating that the electronic properties of the heme group had been irreversibly altered by Aminopyridine 2 in the presence of H_2O_2 (Figure 2D). Similar spectral shifts were seen for Aminopyridine 2 with EPO but not TPO (Supplemental Figure S2), consistent with the enzymatic analysis. The nature of reactive species generated and subsequent alteration of the MPO heme environment is unclear and will require further experimentation, though initial analysis does not suggest an obvious modification to the heme group (data not shown).

Increased MPO activity has been linked to endothelial dysfunction and impaired vasomotor function in humans and preclinical models (Eiserich et al., 2002; Rudolph et al., 2012). Based on previous literature (Zhang et al., 2001), we developed an *ex vivo* model of MPO-dependent vasomotor dysfunction. Rat aorta was dissected and cut into rings that were then incubated in a modified Krebs-Henseleit buffer under various conditions. Incubation with either MPO or H_2O_2 alone did not impair acetylcholine-dependent relaxation, but the combination of both MPO and H_2O_2 resulted in impaired relaxation (Figure 3). MPO and H_2O_2 exposure did not impair smooth muscle cell relaxation in response to the direct nitric oxide donor sodium nitroprusside (not shown), consistent with a direct effect of MPO and H_2O_2 on endothelial function. Aminopyridine 2 dose-dependently inhibited the MPO-dependent endothelial dysfunction while preserving vasomotor function (Figure 3).

We evaluated the pharmacokinetics of Aminopyridine 2 in the mouse, rat, and dog. Low clearance, good oral exposure and high oral bioavailability were observed across all three species (Table 2, Supplemental Figure S3). The pharmacokinetic/pharmacodynamic relationship of Aminopyridine 2 was then evaluated *in vivo* in an induced peritonitis mouse model of acute inflammation. Mice were administered successive intraperitoneal doses of thioglycolate and zymosan A to promote neutrophil infiltration into the peritoneal cavity and degranulation, respectively. Oral administration of 2.5, 25, 50 or 100 mg/kg of Aminopyridine 2 one hour prior to zymosan injection resulted in dose-dependent decreases in 3-chlorotyrosine accumulation in the peritoneal exudate (Figure 4A), along with 24, 62, 74 and 86% decreases in residual plasma MPO activity observed after five hours (Figure 4B). The specificity of these endpoints was confirmed by the lack of detectable MPO activity in the exudate and plasma following the induction of peritonitis in MPO null mice (Figures 4A and 4B). Analysis of terminal plasma Aminopyridine 2 concentrations allowed us to calculate an apparent *in vivo* IC_{50} of 1.4 μM in the peritonitis model (Figure 4C), similar to the human plasma IC_{50} (Figure 2A).

To support chronic studies, we evaluated the potential to deliver Aminopyridine 2 in a food admixture. Aminopyridine 2 was formulated into a western diet (Research Diets D12079B), and mice were fed control diet, diet + 0.0417% (w/w) Aminopyridine 2 (~50 mg/kg/day), or diet + 0.1668% (w/w) Aminopyridine 2 (~200 mg/kg/day) for two weeks. On day 14, peritonitis was induced in the mice, and MPO activity was assessed in both the peritoneal exudate and plasma. Aminopyridine 2 was able to dose-dependently inhibit both accumulation of 3-chlorotyrosine in the peritoneal exudate (Figure 4D) and

JPET Fast Forward. Published on August 3, 2018 as DOI: 10.1124/jpet.118.248435
This article has not been copyedited and formatted. The final version may differ from this version.

plasma MPO activity (Figure 4E), demonstrating that sufficient compound exposure to enable MPO inhibition and long term efficacy studies could be achieved.

Discussion

We screened a library of compounds with the goal of identifying novel mechanism-based irreversible inhibitors and identified 2-aminopyridines as one such class. Our data suggest that these aminopyridines fully and irreversibly inactivate MPO by modifying its heme environment. We demonstrate >500-fold selectivity against TPO with Aminopyridine 2, suggesting an improved selectivity profile for this compound relative to known thiouracil-based inhibitors. Activity against EPO, however, suggests further selectivity profiling is warranted. Additionally, understanding the relevancy of Aminopyridine 2 potentially escaping the active site as a radical species and the likelihood of this posing a safety risk warrants further experimentation. Importantly, the aminopyridines described here potently and dose-dependently inactivated MPO *in vivo* as demonstrated by inhibition of MPO enzymatic activity in plasma and formation of the HOCl-derived biomarker 3-chlorotyrosine in the peritoneum. Aminopyridine 2 also has excellent PK characteristics in rat, mouse and dog, making it a promising tool for evaluating the role of MPO in models of inflammatory disease.

Neutrophil adhesion and degranulation is thought to promote functional changes in the vasculature resulting in impaired vasomotor function and endothelial dysfunction. Upon secretion, MPO is found predominantly in the blood stream where it binds to HDL and the extracellular matrix of blood vessels. Previous data has suggested that vascular MPO can induce endothelial dysfunction and impaired vaso-relaxation (Eiserich et al., 2002). While the precise mechanism is not clear, consumption of endothelial cell-derived nitric oxide and direct oxidative damage to endothelial cells has been implicated. Here we developed an *ex vivo* model of MPO-dependent vasomotor

dysfunction, demonstrating that both MPO and H_2O_2 are required to cause endothelial dysfunction and impair relaxation. Aminopyridine 2 was able to dose-dependently preserve vasomotor function and maintain a normal relaxation response to acetylcholine.

Given its high oral bioavailability, Aminopyridine 2 could be administered by daily oral gavage to support short studies or in food admixtures to support chronic studies. Aminopyridine 2 was effective *in vivo* in an acute model of inflammation (peritonitis). Using two assays of MPO inhibition (peritoneal Cl-Tyr and plasma MPO activity) we demonstrated clear dose-dependent enzymatic inhibition with Aminopyridine 2 by either oral gavage or food admixture. Collectively these data suggest that aminopyridines can be effective inhibitors of MPO *in vivo* and good tools for elucidating the function of MPO in disease models.

Leukocyte-derived oxidants, including those produced by MPO, are associated with inflammatory disease in multiple tissue beds. We focused on MPO as there are significant clinical and preclinical data suggesting a potential role in the pathogenesis of cardiovascular disease and identified Aminopyridine 2 as a potent tool.

Acknowledgements: We would like to thank Samantha Plonsky, Eric Fortier, Jian Hong, Chenhui Zeng, Jay Larrow, and Keith Hoffmaster for contributions to the project and Jason Elliot, Gerry Waters and Jennifer Allport-Anderson for critical review of the manuscript.

Author Contributions

Participated in research design: Marro, Patterson, Lee, Deng, Ren, Axford, Patnaik, Hollis-Symynkywicz, Casson, Custeau, Ames, Loi, Zhang, Honda, Blank, Harrison, Papillon, Hamann, Marcinkeviciene, Regard

Conducted experiments: Patterson, Lee, Ren, Axford, Patnaik, Hollis-Symynkywicz, Casson, Custeau, Ames, Loi, Zhang, Honda, Harrison, Regard

Performed data analysis: Marro, Patterson, Lee, Deng, Ren, Axford, Patnaik, Hollis-Symynkywicz, Casson, Custeau, Ames, Loi, Zhang, Honda, Blank, Harrison, Papillon, Regard

Wrote or contributed to writing the manuscript: Marro, Patterson, Lee, Deng, Ren, Axford, Patnaik, Hollis-Symynkywicz, Ames, Zhang, Blank, Harrison, Papillon, Hamann, Marcinkeviciene, Regard

References

Askari AT, Brennan ML, Zhou X, Drinko J, Morehead A, Thomas JD, Topol EJ, Hazen SL and Penn MS (2003) Myeloperoxidase and plasminogen activator inhibitor 1 play a central role in ventricular remodeling after myocardial infarction. *J Exp Med* **197**:615-624.

Brennan ML, Anderson MM, Shih DM, Qu XD, Wang X, Mehta AC, Lim LL, Shi W, Hazen SL, Jacob JS, Crowley JR, Heinecke JW and Lusis AJ (2001) Increased atherosclerosis in myeloperoxidase-deficient mice. *J Clin Invest* **107**:419-430.

Castellani LW, Chang JJ, Wang X, Lusis AJ and Reynolds WF (2006) Transgenic mice express human MPO -463G/A alleles at atherosclerotic lesions, developing hyperlipidemia and obesity in -463G males. *J Lipid Res* **47**:1366-1377.

Churg A, Marshall CV, Sin DD, Bolton S, Zhou S, Thain K, Cadogan EB, Maltby J, Soars MG, Mallinder PR and Wright JL (2012) Late intervention with a myeloperoxidase inhibitor stops progression of experimental chronic obstructive pulmonary disease. *Am J Respir Crit Care Med* **185**:34-43.

Copeland RA (2005) Evaluation of enzyme inhibitors in drug discovery. A guide for medicinal chemists and pharmacologists. *Methods Biochem Anal* **46**:1-265.

Dong JQ, Varma MV, Wolford A, Ryder T, Di L, Feng B, Terra SG, Sagawa K and Kalgutkar AS (2016) Pharmacokinetics and Disposition of the Thiouracil Derivative PF-06282999, an Orally Bioavailable, Irreversible Inactivator of Myeloperoxidase Enzyme, Across Animals and Humans. *Drug Metab Dispos* **44**:209-219.

Ehrenfeld P, Matus CE, Pavicic F, Toledo C, Nualart F, Gonzalez CB, Burgos RA, Bhoola KD and Figueroa CD (2009) Kinin B1 receptor activation turns on exocytosis of matrix metalloprotease-9 and myeloperoxidase in human neutrophils: involvement of mitogen-activated protein kinase family. *J Leukoc Biol* **86**:1179-1189.

Eiserich JP, Baldus S, Brennan ML, Ma W, Zhang C, Tousson A, Castro L, Lusis AJ, Nauseef WM, White CR and Freeman BA (2002) Myeloperoxidase, a leukocyte-derived vascular NO oxidase. *Science* **296**:2391-2394.

Franck T, Kohnen S, Boudjeltia KZ, Van Antwerpen P, Bosseloir A, Niesten A, Gach O, Nys M, Deby-Dupont G and Serteyn D (2009) A new easy method for specific measurement of active myeloperoxidase in human biological fluids and tissue extracts. *Talanta* **80**:723-729.

Geoghegan KF, Varghese AH, Feng X, Bessire AJ, Conboy JJ, Ruggeri RB, Ahn K, Spath SN, Filippov SV, Conrad SJ, Carpino PA, Guimaraes CR and Vajdos FF (2012) Deconstruction of activity-dependent covalent modification of heme in human neutrophil myeloperoxidase by multistage mass spectrometry (MS(4)). *Biochemistry* **51**:2065-2077.

Haslacher H, Perkmann T, Gruenewald J, Exner M, Endler G, Scheichenberger V, Wagner O and Schillinger M (2012) Plasma myeloperoxidase level and peripheral arterial disease. *Eur J Clin Invest* **42**:463-469.

Johnstrom P, Bergman L, Varnas K, Malmquist J, Halldin C and Farde L (2015) Development of rapid multistep carbon-11 radiosynthesis of the myeloperoxidase

inhibitor AZD3241 to assess brain exposure by PET microdosing. *Nucl Med Biol* **42**:555-560.

Jucaite A, Svenningsson P, Rinne JO, Cselenyi Z, Varnas K, Johnstrom P, Amini N, Kirjavainen A, Helin S, Minkwitz M, Kugler AR, Posener JA, Budd S, Halldin C, Varrone A and Farde L (2015) Effect of the myeloperoxidase inhibitor AZD3241 on microglia: a PET study in Parkinson's disease. *Brain* **138**:2687-2700.

Kaindlstorfer C, Sommer P, Georgievska B, Mather RJ, Kugler AR, Poewe W, Wenning GK and Stefanova N (2015) Failure of Neuroprotection Despite Microglial Suppression by Delayed-Start Myeloperoxidase Inhibition in a Model of Advanced Multiple System Atrophy: Clinical Implications. *Neurotox Res* **28**:185-194.

Klebanoff SJ (2005) Myeloperoxidase: friend and foe. *J Leukoc Biol* **77**:598-625.

Kutter D, Devaquet P, Vanderstocken G, Paulus JM, Marchal V and Gothot A (2000) Consequences of total and subtotal myeloperoxidase deficiency: risk or benefit ? *Acta Haematol* **104**:10-15.

Marsche G, Zimmermann R, Horiuchi S, Tandon NN, Sattler W and Malle E (2003) Class B scavenger receptors CD36 and SR-BI are receptors for hypochlorite-modified low density lipoprotein. *J Biol Chem* **278**:47562-47570.

McMillen TS, Heinecke JW and LeBoeuf RC (2005) Expression of human myeloperoxidase by macrophages promotes atherosclerosis in mice. *Circulation* **111**:2798-2804.

Nussbaum C, Klinke A, Adam M, Baldus S and Sperandio M (2013) Myeloperoxidase: a leukocyte-derived protagonist of inflammation and cardiovascular disease. *Antioxid Redox Signal* **18**:692-713.

Rudolph TK, Wipper S, Reiter B, Rudolph V, Coym A, Detter C, Lau D, Klinke A, Friedrichs K, Rau T, Pekarova M, Russ D, Knoll K, Kolk M, Schroeder B, Wegscheider K, Andresen H, Schwedhelm E, Boeger R, Ehmke H and Baldus S (2012) Myeloperoxidase deficiency preserves vasomotor function in humans. *Eur Heart J* **33**:1625-1634.

Ruggeri RB, Buckbinder L, Bagley SW, Carpino PA, Conn EL, Dowling MS, Fernando DP, Jiao W, Kung DW, Orr ST, Qi Y, Rocke BN, Smith A, Warmus JS, Zhang Y, Bowles D, Widlicka DW, Eng H, Ryder T, Sharma R, Wolford A, Okerberg C, Walters K, Maurer TS, Zhang Y, Bonin PD, Spath SN, Xing G, Hepworth D, Ahn K and Kalgutkar AS (2015) Discovery of 2-(6-(5-Chloro-2-methoxyphenyl)-4-oxo-2-thioxo-3,4-dihydropyrimidin-1(2H)-yl)acet amide (PF-06282999): A Highly Selective Mechanism-Based Myeloperoxidase Inhibitor for the Treatment of Cardiovascular Diseases. *J Med Chem* **58**:8513-8528.

Schultz J and Kaminker K (1962) Myeloperoxidase of the leucocyte of normal human blood. I. Content and localization. *Arch Biochem Biophys* **96**:465-467.

Shao B, Oda MN, Oram JF and Heinecke JW (2010) Myeloperoxidase: an oxidative pathway for generating dysfunctional high-density lipoprotein. *Chem Res Toxicol* **23**:447-454.

Stefanova N, Georgievska B, Eriksson H, Poewe W and Wenning GK (2012) Myeloperoxidase inhibition ameliorates multiple system atrophy-like degeneration in a transgenic mouse model. *Neurotox Res* **21**:393-404.

Sugiyama S, Kugiyama K, Aikawa M, Nakamura S, Ogawa H and Libby P (2004) Hypochlorous acid, a macrophage product, induces endothelial apoptosis and tissue factor expression: involvement of myeloperoxidase-mediated oxidant in plaque erosion and thrombogenesis. *Arterioscler Thromb Vasc Biol* **24**:1309-1314.

Tiden AK, Sjogren T, Svensson M, Bernlind A, Senthilmohan R, Auchere F, Norman H, Markgren PO, Gustavsson S, Schmidt S, Lundquist S, Forbes LV, Magon NJ, Paton LN, Jameson GN, Eriksson H and Kettle AJ (2011) 2-thioxanthines are mechanism-based inactivators of myeloperoxidase that block oxidative stress during inflammation. *J Biol Chem* **286**:37578-37589.

Wang Y, Rosen H, Madtes DK, Shao B, Martin TR, Heinecke JW and Fu X (2007) Myeloperoxidase inactivates TIMP-1 by oxidizing its N-terminal cysteine residue: an oxidative mechanism for regulating proteolysis during inflammation. *J Biol Chem* **282**:31826-31834.

Zhang C, Patel R, Eiserich JP, Zhou F, Kelpke S, Ma W, Parks DA, Darley-Usmar V and White CR (2001) Endothelial dysfunction is induced by proinflammatory oxidant hypochlorous acid. *Am J Physiol Heart Circ Physiol* **281**:H1469-1475.

Zheng W, Warner R, Ruggeri R, Su C, Cortes C, Skoura A, Ward J, Ahn K, Kalgutkar A, Sun D, Maurer TS, Bonin PD, Okerberg C, Bobrowski W, Kawabe T, Zhang Y, Coskran T, Bell S, Kapoor B, Johnson K and Buckbinder L (2015) PF-1355, a

mechanism-based myeloperoxidase inhibitor, prevents immune complex vasculitis and anti-glomerular basement membrane glomerulonephritis. *J Pharmacol Exp Ther* **353**:288-298.

Footnotes:

Figure Legends

Figure 1: The MPO catalytic cycle and chemical structures of interest

A) “Native” MPO reacts with H_2O_2 to form compound I, a highly oxidative and reactive species. Compound I can return to its native state by reacting with a halogen such as chloride, or via two electron reductions with compound II as an intermediate. B) The structures are shown for Aminopyridines 1 and 2 and advanced thiouracils.

Figure 2: Aminopyridine 2 irreversibly inhibits MPO

A) Aminopyridine 2 was incubated with human MPO in phosphate buffer (peroxidation) or human plasma as described in the materials and methods. MPO activity in the presence of H_2O_2 and Amplex Red was measured by fluorescence. Aminopyridine 2 inhibited MPO activity with an apparent IC_{50} of 0.16 µM (blue squares), which shifted to 1.9 µM in the presence of human plasma (red circles). B) Aminopyridine 2 (or DMSO vehicle) was incubated with human MPO and H_2O_2, followed by dialysis and dilution. Aminopyridine 2-dependent inhibition could not be reversed suggesting irreversible inhibition. C) K_{obs} values plotted as a function of Aminopyridine 2 concentration allowed determination of k_{inact} and K_i values. D) The incubation of MPO, H_2O_2 and Aminopyridine 2 results in a shift of the Soret peak and formation of a new peak at 624 nm, consistent with a modification of MPO at or near the heme prosthetic group.

Figure 3: Aminopyridine 2 prevents MPO-dependent endothelial dysfunction *ex vivo*

Rat aortic rings were preincubated with MPO, +/- H_2O_2 and +/- Aminopyridine 2. The ability of the rings to constrict in response to phenylephrine and then relax in response

to acetylcholine (Ach) was determined *ex vivo* in organ baths. Incubation of the rings with either MPO alone or H_2O_2 alone had no effect, while the combination resulted in an inability to respond to acetylcholine. The addition of Aminopyridine 2 dose-dependently blocked the MPO-dependent vasomotor dysfunction.

Figure 4: Acute and chronic administration of Aminopyridine 2 inhibits MPO activity in a mouse model of peritonitis.

Aminopyridine 2 was dosed to mice orally (n=8-12) just prior to zymosan A administration and MPO activity in the peritoneal exudate and plasma was measured. Aminopyridine 2 dose-dependently inhibited 3-chlorotyrosine accumulation in the peritoneal exudate (A) and also inhibited residual MPO activity in the plasma 5 hours post-dose (B). There was an inverse relationship between total plasma Aminopyridine 2 concentration and plasma MPO activity, with the apparent *in vivo* IC_{50} estimated to be 1.4 µM (C). Aminopyridine 2 was formulated as a food admixture and mice were fed *ad lib* for 14 days. Aminopyridine 2 dose-dependently inhibited MPO activity in both peritoneal exudate by Cl-Tyr/Tyr ratio (D) and plasma by residual MPO activity (E). Data are presented as mean ± SEM and statistics were performed using one-way ANOVA. *p<0.05 represents significance when compared to vehicle.

JPET Fast Forward. Published on August 3, 2018 as DOI: 10.1124/jpet.118.248435
This article has not been copyedited and formatted. The final version may differ from this version.

Table 1: *In vitro* pharmacology data for Aminopyridine 1 and 2

Aminopyridine Compound	MPO IC_{50} (μM)	MPO k_{inact}/K_i ($M^{-1}s^{-1}$)	MPO k_3/k_4	MPO dialysis (% recovered activity)	TPO IC_{50} (μM)	TPO selectivity (fold)
1	0.45	14,000	57	42%	>100	>222
2	0.16	76,500	11	8%	>100	>588

Values were determined as described in the materials and methods section and presented as the geometric mean of at least three independent experiments.

Table 2: Summary of pharmacokinetic data for Aminopyridine 2 in preclinical species

Species	Oral. Cmax @10mg/kg (nM)	Oral Tmax @10mg/kg (hrs)	Oral AUC 0-∞ (nM*hr/mL)	CLp (mL/min/kg)	Vdss (L/kg)	$T_{1/2}$ (hrs)	Oral F (%)
Mouse	11884	1.3	58440	4.5	0.7	1.9	51
Rat	20844	0.4	133162	4.5	1.3	4.1	~100
Dog	19486	2.3	335615	1.9	0.9	7	~100

The pharmacokinetics of Aminopyridine 2 in mice, rats and dogs are summarized. Aminopyridine 2 concentrations were measured from plasma collected at specific time points and pharmacokinetic parameters were calculated. All data are reported as the mean (n=2-3). Cmax = maximal concentration, Tmax = time to maximal concentration, AUC = area under the curve, CLp = plasma clearance, Vdss = volume of distribution, $T_{1/2}$ = half-life, Oral F = oral bioavailibility

Figure 1

A

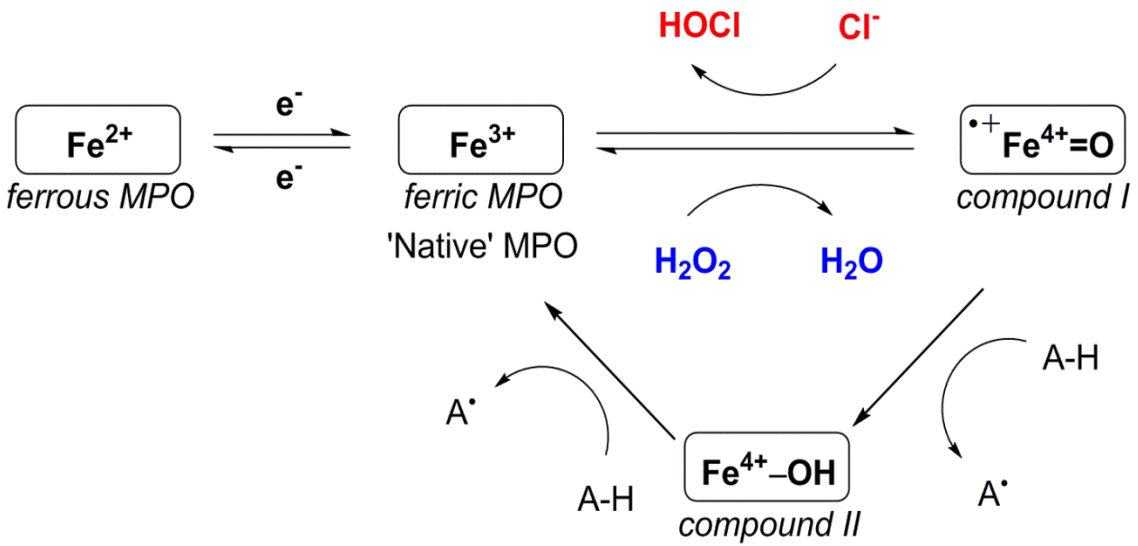

B

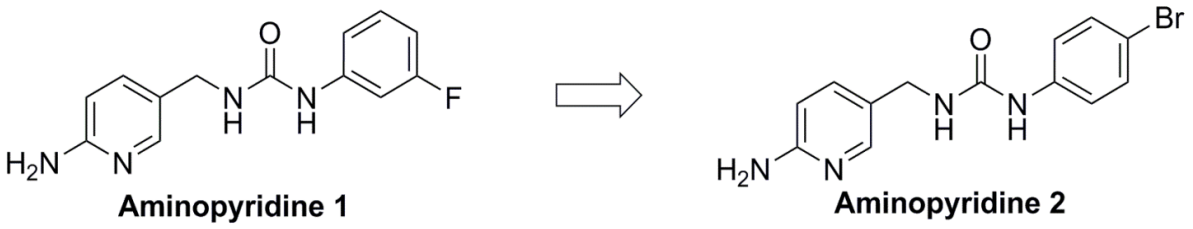

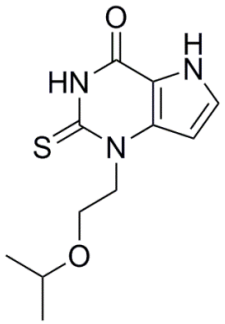

AZD3241

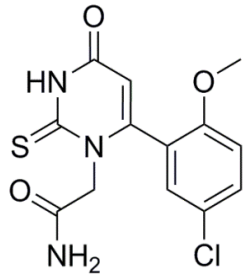

PF-06282999

Figure 2

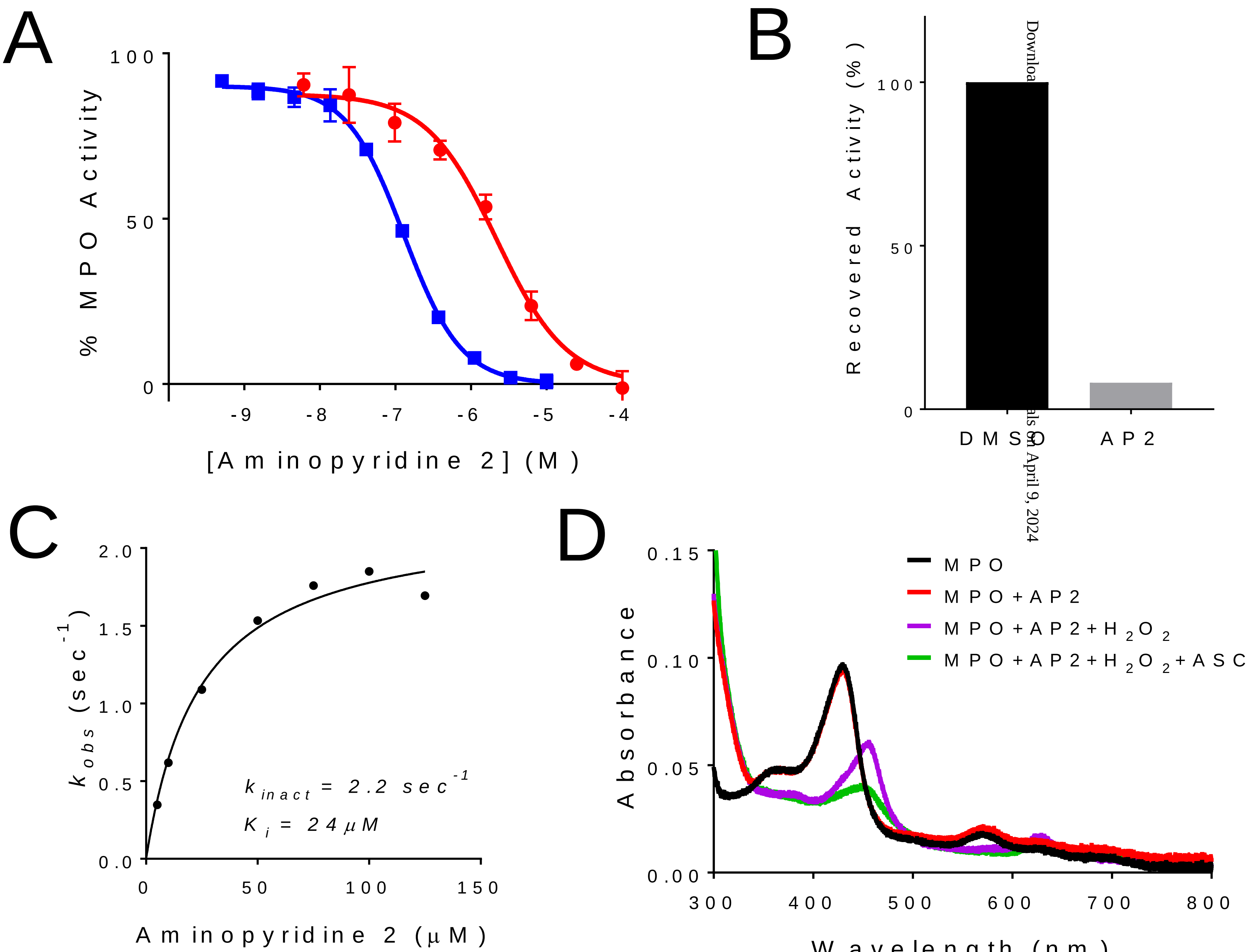

Figure 3

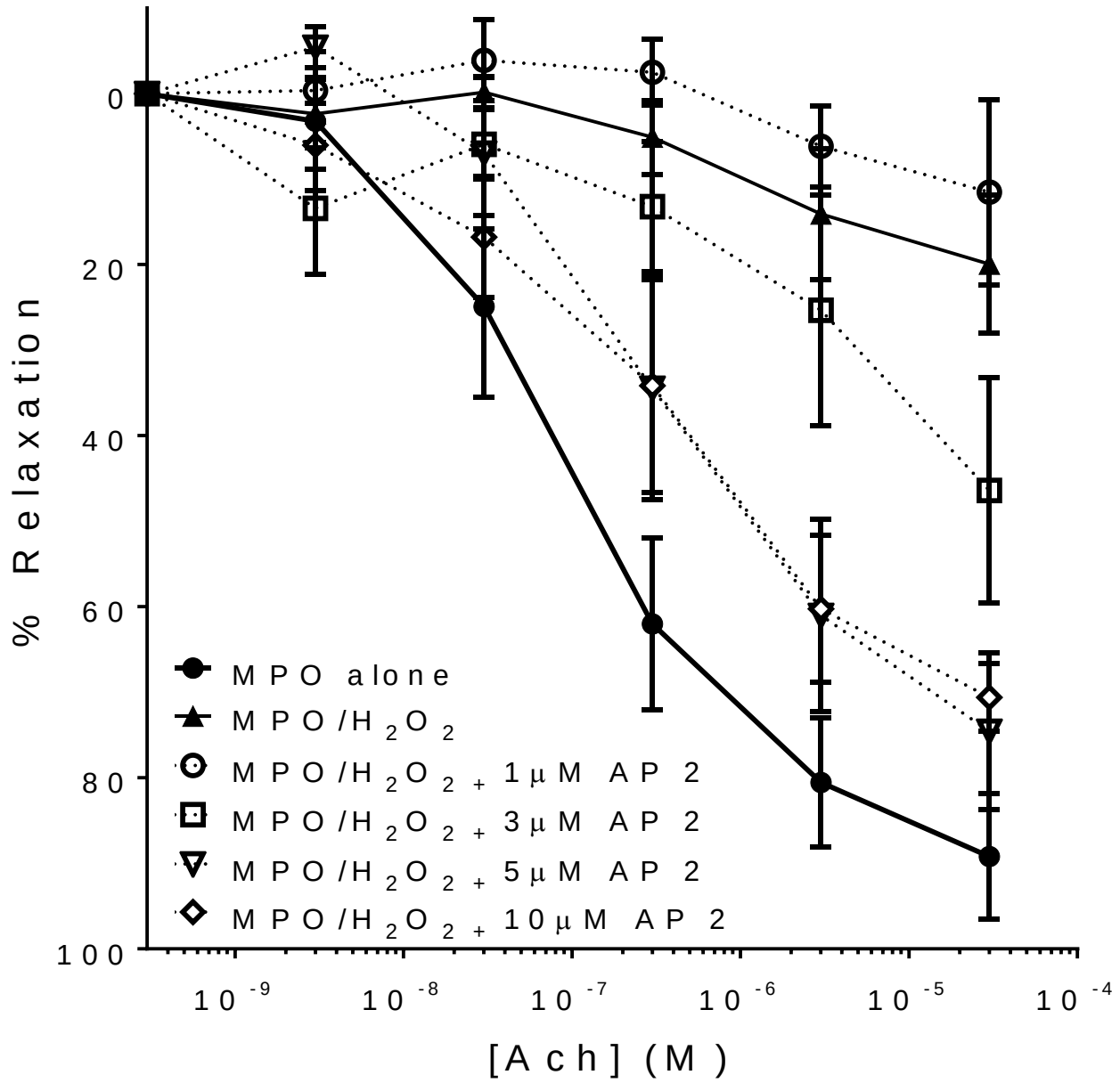

Figure 4